SLEEPJ, 2019, 1–12

doi: 10.1093/sleep/zsz062
Advance Access Publication Date: 7 March, 2019
Original Article

ORIGINAL ARTICLE

Brain atrophy in Parkinson's disease with polysomnography-confirmed REM sleep behavior disorder

Shady Rahayel[1–3,†], Malo Gaubert[1,2,†], Ronald B. Postuma[1,4], Jacques Montplaisir[1,5], Julie Carrier[1,3,6], Oury Monchi[3,7,8], David Rémillard-Pelchat[1,2], Pierre-Alexandre Bourgouin[1,2], Michel Panisset[9], Sylvain Chouinard[9], Sven Joubert[3,6] and Jean-François Gagnon[1–3,*]

[1]Centre for Advanced Research in Sleep Medicine, Hôpital du Sacré-Cœur de Montréal, Montreal, Canada, [2]Department of Psychology, Université du Québec à Montréal, Montreal, Canada, [3]Research Centre, Institut universitaire de gériatrie de Montréal, Montreal, Canada, [4]Department of Neurology, Montreal General Hospital, Montreal, Canada, [5]Department of Psychiatry, Université de Montréal, Montreal, Canada, [6]Department of Psychology, Université de Montréal, Montreal, Canada, [7]Department of Radiology, Radio-Oncology, and Nuclear Medicine, Université de Montréal, Montreal, Canada, [8]Departments of Clinical Neurosciences, Radiology, and Hotchkiss Brain Institute, University of Calgary, Calgary, Canada and [9]Unité des troubles du mouvement André-Barbeau, Centre Hospitalier de l'Université de Montréal, Montreal, Canada

Work Performed: Centre for Advanced Research in Sleep Medicine, Hôpital du Sacré-Cœur de Montréal, and Department of Psychology, Université du Québec à Montréal, Montreal, Canada

[†]Shady Rahayel and Malo Gaubert share first authorship.

[*]Corresponding author. Jean-François Gagnon, Centre for Advanced Research in Sleep Medicine, Hôpital du Sacré-Cœur de Montréal, Centre Intégré Universitaire de Santé et Services Sociaux du Nord-de-L'Ile de Montréal, 5400 Boul. Gouin ouest, Montreal, Quebec, Canada H4J 1C5. Email: gagnon.jean-francois.2@uqam.ca.

Abstract

We aimed to investigate cortical and subcortical brain alterations in people with Parkinson's disease with polysomnography-confirmed rapid eye movement (REM) sleep behavior disorder (RBD). Thirty people with Parkinson's disease, including 15 people with RBD, were recruited and compared with 41 healthy controls. Surface-based cortical and subcortical analyses were performed on T1-weighted images to investigate thickness and shape abnormalities between groups, and voxel-based and deformation-based morphometry were performed to investigate local volume. Correlations were performed in patients to investigate the structural correlates of motor activity during REM sleep. People with RBD showed cortical thinning in the right perisylvian and inferior temporal cortices and shape contraction in the putamen compared with people without RBD. Compared with controls, people with RBD had extensive cortical thinning and volume loss, brainstem volume was reduced, and shape contraction was found in the basal ganglia and hippocampus. In comparison to controls, people without RBD showed more restricted thinning in the sensorimotor, parietal, and occipital cortices, reduced volume in the brainstem, temporal and more posterior areas, and shape contraction in the pallidum and hippocampus. In Parkinson's disease, higher tonic and phasic REM sleep motor activity was associated with contraction of the thalamic surface, extensive cortical thinning, and subtle volume reduction in the middle temporal gyrus. In Parkinson's disease, the presence of RBD is associated with extensive cortical and subcortical abnormalities, suggesting more severe neurodegeneration in people with RBD. This provides potential neuroanatomical correlates for the more severe clinical phenotype reported in people with Parkinson's disease with RBD.

Statement of Significance

The presence of rapid eye movement (REM) sleep behavior disorder (RBD) in Parkinson's disease (PD) is associated with a more severe and aggressive clinical phenotype. Previous studies investigating brain structural alterations in people with PD with RBD had methodological limitations such as the lack of polysomnography, the use of uncorrected statistical thresholds, or the absence of a healthy control group to interpret the results. In this study, we overcame these limitations and, for the first time, performed surface-based structural analyses to investigate the abnormalities in cortical thickness and subcortical shape associated with RBD. People with PD with RBD had extensive cortical abnormalities and shape contraction in the putamen. REM sleep without atonia was also associated in PD with abnormal thalamic shape, extensive cortical thinning, and subtle volume reduction in temporal region. Our study showed that surface-based cortical and subcortical investigations made it possible to reveal additional structural abnormalities in people with PD-RBD and PD-nRBD beyond those that can be detected using volume-based investigations alone.

Key words: REM sleep behavior disorder; Parkinson's disease; Structural MRI; cortical thickness

Submitted: 6 November, 2018; **Revised:** 20 January, 2019

Introduction

Rapid eye movement (REM) sleep behavior disorder (RBD) is characterized by abnormal muscle tone and motor manifestations during REM sleep [1]. RBD affects 33% to 46% of people with Parkinson's disease (PD) according to studies using polysomnography (PSG) [2, 3], which is mandatory for RBD diagnosis [1]. Within PD itself, the presence of RBD is associated with more severe clinical symptoms, mild cognitive impairment (MCI), poorer prognosis, and cerebral functional alterations [4–6]. Moreover, a substantial proportion of people with PD show REM sleep without atonia (RSWA) but do not meet the criteria for RBD diagnosis [2, 3]. In PD, the severity of RSWA has been associated to poorer cognitive performance [6], suggesting that RSWA could be a marker of neurodegeneration in this population.

Few studies have used voxel-based morphometry (VBM) to investigate RBD-related gray matter abnormalities in PD, with the most consistent finding being volume loss in the temporal lobes but with other findings including change in the cingulate cortex, posterior regions, and thalamus [7–11]. Another study used deformation-based morphometry (DBM), a technique shown to detect volume changes occurring in PD with better accuracy [12], and found abnormal volume in several cortical (anterior cingulate, olfactory areas) and subcortical (brainstem, cerebellum, thalamus, putamen, amygdala) regions in people with PD with RBD [13]. However, these studies have some methodological limitations, notably the use of screening questionnaires for RBD diagnosis [10, 11, 13], the use of statistical thresholds uncorrected for multiple comparisons [8, 10, 11], and absence of a healthy control group [10]. Furthermore, the techniques (VBM or DBM) used for analysis were limited by voxel-based resolution, resulting in a partial overview of structural abnormalities in this population. Recently, surface-based investigation of cortical thickness and subcortical shape showed increased sensitivity to detect gray matter brain structural alterations in people with idiopathic RBD [14–17].

Here, we performed whole-brain mapping of cortical and subcortical tissues in people with PD with definite RBD (PD-RBD), people with PD without RBD (PD-nRBD), and controls using surface-based cortical thickness analysis, VBM and DBM (for the purpose of replicating previous studies described above), and subcortical shape and volume analyses. We predicted that people with PD-RBD would present with more severe and extensive brain atrophy compared to people with PD-nRBD and controls. We also predicted that higher tonic and phasic REM sleep motor activity (or RSWA) would associate with cortical and subcortical structural alterations in people with PD.

Methods

Participants

People with PD were recruited at the Department of Neurology of the Montreal General Hospital and the *Unité des troubles du mouvement André-Barbeau* of the *Centre Hospitalier de l'Université de Montréal*. They underwent PSG, neurological, neuropsychological, and magnetic resonance imaging (MRI) examinations. Inclusion criteria were: (1) diagnosis of parkinsonism with idiopathic PD as its most likely cause [18], (2) age from 45 to 85 years, (3) PD duration (diagnosis) ≤ 10 years, and (4) Hoehn and Yahr stage ≤ 3. Exclusion criteria were: (1) causes of parkinsonism other than PD, (2) dementia according to neuropsychological assessment and neurological exam and based on the Diagnostic and Statistical Manual of Mental Disorders, Fifth Edition (DSM-5) criteria [19], (3) major psychiatric disorder (including untreated major depression, schizophrenia, or bipolar disorder) according to DSM-5 criteria [19], (4) respiratory event index (number of apnea and hypopnea events per hour of sleep) > 20, (5) history of head injury, stroke, brain tumor, cerebrovascular disease, or chronic obstructive pulmonary disease, and (6) abnormal EEG features suggesting epilepsy. Controls without PD, RBD, or MCI were recruited from the general population through newspaper advertisements or by word of mouth. All controls were subjected to similar exclusion criteria as people with PD.

Standard protocol approval, registration, and patient consent

Research protocols were approved by the ethics committees of the *CIUSSS-NÎM – Hôpital du Sacré-Cœur de Montréal* and the *Comité mixte d'éthique de la recherche du Regroupement Neuroimagerie Québec*, and all participants gave their informed written consent to participate.

Polysomnography

All patients underwent one night in the sleep laboratory at the Centre for Advanced Research in Sleep Medicine of the *CIUSSS-NÎM – Hôpital du Sacré-Cœur de Montréal*. PSG recording included two standard electrode derivations for monitoring EEG activity during sleep (C3-A2 and O2-A1), left and right electrooculograms, and submental EMG. Oral and nasal airflow and thoracic and abdominal movements were recorded, and pulse oximetry was performed to measure the respiratory event index. Sleep stages were scored according to standard criteria [20, 21]. REM sleep stage and chin EMG (tonic and phasic) activity during REM sleep were identified and quantified as described previously [20]. Abnormal muscle activity during REM sleep was established when chin tonic EMG activity exceeded 30% of total REM sleep time or when chin phasic EMG activity exceeded 15% of total REM sleep time [20]. RBD was diagnosed (J.M. and J.-F.G.) according to the International Classification of Sleep Disorders, Third Edition [1]. People with PD were classified into PD subgroups having RBD (PD-RBD) or not (PD-nRBD).

Neurological and neuropsychological examinations

Patients underwent neurological examination conducted by a movement disorder specialist (R.B.P.) and met clinical criteria for PD [18]. Motor symptoms were quantified in the "ON" state using the Unified Parkinson's Disease Rating Scale, Part III (UPDRS-III) [22]. A neuropsychological assessment was performed in patients and controls to assess performance in five cognitive domains: attention, executive functions, episodic learning and memory, visuospatial abilities, and language. MCI was diagnosed according to the following criteria: (1) evidence of subjective cognitive complaints during semi-structured interview by the patient, the spouse, or an informant, or using the Cognitive Failures Questionnaire [23]; (2) evidence of objective cognitive decline through a neuropsychological assessment, with impaired performance defined as a score at

least 1.5 SD below the standardized mean on at least 2 tasks within a single cognitive domain; (3) absence of significant decline in daily living functioning; (4) absence of dementia; and (5) cognitive deficits not solely explained by medication or other medical conditions [24, 25]. The cognitive tests and normative data are described in detail in a previous publication [25].

Magnetic resonance imaging

MRI data acquisition

All participants underwent MR imaging using a 3-T Siemens TrioTIM scanner (Siemens, Erlangen, Germany) with a 12-channel head matrix coil at the *Unité de Neuroimagerie Fonctionnelle* of the *Institut universitaire de gériatrie de Montréal*. High-resolution T1-weighted images were obtained using magnetization-prepared rapid acquisition with gradient-echo (MP-RAGE) sequence with the following parameters: repetition time 2.3 s, echo time 2.91 ms, inversion time 900 ms, 9-degree flip angle, 160 slices, 256 × 240 mm field of view, 256 × 240 matrix resolution (voxel size: 1 × 1 × 1 mm), and 240 Hz/Px bandwidth.

VBM, DBM, and surface-based cortical thickness processing

To investigate cortical and subcortical structural abnormalities, we conducted VBM, DBM, and surface-based cortical thickness analysis. VBM was performed in order to compare our findings to previous structural studies conducted between people with PD with and without RBD, which used VBM. We also performed DBM since it was shown to detect with better accuracy the structural abnormalities found in PD [12], including in the brainstem in people with RBD [13]. Surface-based cortical thickness analysis was also conducted to investigate with increased precision the local changes occurring in the cerebral cortex; this technique was found to reveal more alterations in people with idiopathic RBD than when using volume-based investigations only [14, 15].

Cortical processing for surface-based cortical thickness analysis, VBM, and DBM was conducted using Computational Anatomy Toolbox (CAT12, Jena University Hospital, Germany; release 1254; www.neuro.uni-jena.de/cat/index.html#SBM) for SPM12 (Wellcome Trust Centre for Neuroimaging, London, UK; release 6906). As a first step, VBM processing was performed, which included spatial registration to a reference template within MNI space using DARTEL; tissue classification into gray matter, white matter, and CSF; and bias correction of intensity nonuniformities. Gray matter maps were then modulated (i.e. scaled by the volume changes due to spatial registration). Normalized modulated images were then smoothed using an 8 mm full width at half maximum (FWHM) kernel. An analysis mask was also generated to restrict the analysis to gray matter voxels only by calculating and thresholding at 0.3 the mean image of individual normalized gray matter maps. Total intracranial volume (TIV) was calculated using the "Tissue Volumes Utility" tool in SPM12.

DBM processing was based on the VBM pipeline [26]. Each voxel transformation from native to template space was calculated during normalization (Jacobian determinant), yielding a matrix in which each voxel was coded with a value representing expansion (>1) or contraction (<1). Individual Jacobian determinants were then normalized to MNI space, and an 8 mm FWHM smoothing kernel was applied to the resulting images. As part of the VBM processing pipeline, white matter segmentation maps were also normalized to MNI space. Both normalized gray matter and white matter maps were then averaged, and a threshold of 0.3 was applied to the resulting maps. Finally, the logical disjunction for the two resulting images was calculated to create the analysis mask, which included whole-brain gray and white matter voxels.

Surface-based cortical thickness analysis was performed using the segmented images that were generated as part of the VBM processing pipeline. Briefly, cortical thickness was calculated as the distance between gray surfaces using VBM segmentation information. Data were then topologically corrected, spherically mapped, and spherically registered. Resulting images were normalized to standard space (MNI). Normalized maps were then smoothed using a 15 mm kernel.

Subcortical shape and volume processing

Vertex-based subcortical shape processing was conducted using FSL-FIRST 5.0.9 (Oxford Centre for Functional MRI of the Brain, Oxford, UK) [16]. The following subcortical structures were available as surface models for segmentation: the nucleus accumbens, amygdala, caudate nucleus, hippocampus, pallidum, putamen, and thalamus. Following rigid-body alignment, all structures were normalized to MNI space before vertex-based shape analysis. We also obtained global volumes in mm^3 for each subcortical structure by defining the boundaries and filling the interior using optimal parameters for each structure [16]. Global volume values for each subcortical structure were then adjusted for head size by using the scaling factor generated from SIENAX [27], part of FSL [28]. These normalized global volume values were then used as input data for subcortical volume analysis between PD subgroups and controls.

Statistical analysis

Demographic and clinical variables

Statistical analyses were performed using IBM SPSS Statistics, version 22.0 (IBM Corp., Armonk, NY). Continuous variables were compared between PD-RBD, PD-nRBD, and controls using one-way analysis of variance or Kruskal–Wallis *H* test for normally and non-normally distributed variables, respectively. Pairwise differences were investigated using Student's *t*-tests and Mann–Whitney *U* tests. Between-group differences for categorical variables were assessed using the Freeman–Halton extension of Fisher's exact probability test and χ^2 (chi-squared) tests for pairwise comparisons.

Cortical and subcortical analysis

Between-group differences (HC vs. PD-nRBD vs. PD-RBD) in surface-based cortical thickness, VBM, and DBM were assessed using general linear modeling (GLM) in SPM12 and using FSL for vertex-based subcortical shape analysis. Age, gender, and education (and TIV for VBM analysis) were included as covariates. Since the presence of RBD in PD is associated with MCI and more severe motor symptoms, a second GLM was used to directly compare PD subgroups, with age, gender, education, MCI status, and UPDRS-III (and TIV for VBM analysis) included as covariates in order to isolate the impact of RBD from cognitive status and motor symptoms. TIV was not added as a covariate in subcortical shape analysis since analyses were conducted in the MNI152 space. To avoid spurious results, only clusters

comprising at least 50 voxels or vertices were retained for further interpretation. Similarly, in the subcortical shape analysis, only clusters that resulted in at least a 5% change in the global shape structure were considered significant. A threshold of $p < 0.05$ corrected for multiple comparisons (family-wise error, FWE) using threshold-free cluster enhancement was applied in SPM12 (http://dbm.neuro.uni-jena.de/tfce/) and FSL Randomize with 5000 permutations [29, 30].

Subcortical volumetric analysis

Multivariate analysis of covariance (MANCOVA) was performed to investigate the presence of volume differences between PD-RBD, PD-nRBD, and controls, with normalized global subcortical volumes as dependent variables, group (PD-RBD, PD-nRBD, and controls) as fixed factor, and age, gender, and education as covariates. Separate univariate analyses of covariance (ANCOVA) were then performed to identify the subcortical structure where volume changes occurred using a Bonferroni-corrected threshold to correct for multiple comparisons (14 comparisons, $p < 0.0036$). Post hoc tests were conducted in significant structures to identify the contrasts where volume changes occurred. TIV was not added as a covariate in either analysis since subcortical volume values were scaled for head size during processing. We also conducted the analysis between PD-RBD and PD-nRBD groups only, with age, gender, education, MCI status, and UPDRS-III total score as covariates in order to verify whether the volume changes remained significant (14 comparisons, $p < 0.0036$) after accounting for cognitive status and motor symptom severity.

Regression analysis with EMG activity

Regression analyses were performed in the whole group of people with PD (since some people with PD-nRBD present with abnormally elevated EMG activity during REM sleep without meeting RBD diagnostic criteria) between cortical and subcortical metrics and tonic and phasic REM sleep motor activity. Age, gender, education, UPDRS-III, and MCI status (and TIV for VBM analysis) were used as covariates. Results were considered significant at $p < 0.05$ FWE-corrected for multiple comparisons for cortical and subcortical shape analyses. A statistical threshold of $p < 0.0018$ was used for correlations between subcortical volumes and EMG activity (corrected for multiple comparisons, 28 comparisons).

Results

Demographic and clinical characteristics

Thirty-six people with PD were initially recruited. Thirty people with PD met inclusion criteria: mean age (SD), 64.8 (8.3) years; gender, 15 men (50%); mean education, 14.9 (3.8) years; mean PD duration, 3.8 (2.7) years; mean UPDRS-III total "ON" score, 20.8 (9.5); mean tonic REM sleep motor activity, 38.4% (36.6); mean phasic REM sleep motor activity, 28.5% (19.3); 27 patients (90%) taking levodopa; mean levodopa dosage, 536.5 (283.1) mg; 13 patients (43%) taking dopamine agonists; 12 patients (40%) with MCI) and 41 controls (mean age (SD), 63.3 (8.1) years; gender, 25 men (61%); mean education, 14.6 (4.1) years. Fifteen people with PD met definite RBD diagnostic criteria (PD-RBD) and 15 did not (PD-nRBD). As for controls, 30 underwent PSG recording to exclude RBD, whereas the remaining controls ($n = 11$) did not report RBD symptoms at interview. We performed the same analyses excluding these 11 controls and found similar results, except for subcortical shape analysis (see below for details). Demographic and clinical characteristics are presented in Table 1. There were no significant differences between groups, although people with PD-RBD had nonsignificant increases in age (66.7 vs. 63.1), UPDRS-III total score (24.1 vs. 17.6), and diagnosis of MCI (53% vs. 27%). As expected, people with PD-RBD showed increased tonic and phasic REM sleep motor activity compared with people with PD-nRBD.

Surface-based cortical thickness analysis

People with PD-RBD showed cortical thinning compared with people with PD-nRBD in the right perisylvian areas (caudal sensorimotor, supramarginal, and superior temporal cortices) and the temporal cortex (temporal pole and inferior temporal

Table 1. Demographic and clinical characteristics of participants

Variable	PD-RBD	PD-nRBD	Controls	*P*
Age, y	66.7 (7.6)	63.1 (8.9)	63.3 (8.1)	0.36*
Men, *n* (%)	10 (67)	5 (33)	25 (61)	0.14†
Education, y	14.2 (3.6)	15.7 (3.9)	14.6 (4.1)	0.56*
PD duration, diagnosis, y	3.9 (2.9)	3.7 (2.6)	–	0.85‡
% tonic REM sleep motor activity	56.3 (33.8)	23.0 (32.5)	–	**0.01**§
% phasic REM sleep motor activity	38.6 (17.3)	19.8 (16.9)	–	**0.004**§
UPDRS-III, total "ON" state	24.1 (10.0)	17.6 (8.5)	–	0.08‡
Levodopa equivalent dosage, mg	625.2 (347.1)	447.8 (171.5)	–	0.65§
Levodopa use, %	87	93	–	0.54‖
Dopamine agonist use, %	47	40	–	0.71‖
MCI, %	53	27	–	0.14‖

Data are presented as mean (SD). Bold values represent significant between-group differences.
MCI = mild cognitive impairment; PD-RBD = Parkinson's disease with REM sleep behavior disorder; PD-nRBD = PD without RBD; UPDRS-III = Unified Parkinson's Disease Rating Scale, Part III.
*Analysis of variance.
†Fisher–Freeman–Halton exact test for contingency.
‡Student's *t*-test.
§Mann–Whitney *U* test.
‖Chi-squared test.

Table 2. Results of surface-based cortical thickness analysis

Region with thickness abnormalities*	Hemisphere	Cluster size, mm²	MNI coordinates			P
			x	y	z	
PD-RBD < PD-nRBD						
Inferior temporal gyrus	Right	1415	47	−40	−21	0.034
Superior temporal gyrus	Right	1772	66	−30	11	0.038
PD-RBD < Controls						
Fusiform gyrus	Right	23 256	29	−63	−10	<0.001
Amygdala	Left	19 069	−27	−4	−27	<0.001
Medial orbitofrontal gyrus	Left	178	−15	40	−24	0.015
Lateral orbitofrontal gyrus	Left	63	−25	16	−24	0.042
PD-nRBD < Controls						
Postcentral gyrus	Right	5307	29	−26	49	0.002
Middle cingulate cortex	Left	5430	−8	−5	41	0.003
Fusiform gyrus	Right	121	25	−85	−10	0.045
Correlation with % of tonic REM sleep motor activity in PD						
Superior temporal gyrus	Right	14 782	65	−17	5	0.007
Postcentral gyrus	Left	7179	−48	−19	58	0.024
Lateral orbitofrontal gyrus	Right	406	30	20	−22	0.045
Correlation with % of phasic REM sleep motor activity in PD						
Middle temporal gyrus	Left	4185	−62	−16	−16	0.028
Precentral gyrus	Right	910	55	6	19	0.032
Inferior parietal gyrus	Left	268	−39	−77	30	0.046
Supramarginal gyrus	Left	137	−30	−49	42	0.048

Results are corrected for multiple comparisons with FWE at $p < 0.05$, with age, gender, and education as covariates. UPDRS-III and MCI status were included as covariates for comparisons between PD-RBD and PD-nRBD subgroups. FWE = family-wise error; MCI = mild cognitive impairment; MNI = Montreal Neurological Institute; PD-RBD = Parkinson's disease with REM sleep behavior disorder; PD-nRBD = PD without RBD; UPDRS-III = Unified Parkinson's Disease Rating Scale, Part III.
*Labels correspond to the location of the cluster's peak voxel.

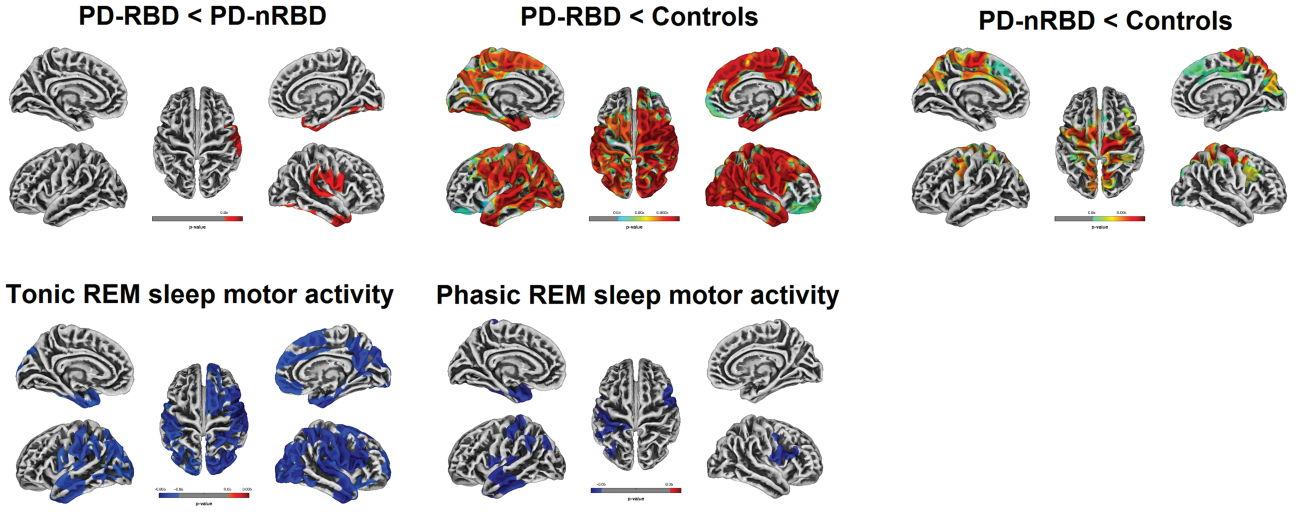

Figure 1. Results of surface-based cortical thickness analysis. Cortical thickness in PD-RBD vs PD-nRBD (top left), PD-RBD vs controls (top center), and PD-nRBD vs controls (top right). Correlations between cortical thickness and percentage of tonic (bottom left) and phasic (bottom center) REM sleep motor activity in people with PD. Results are presented at $p < 0.05$ corrected for multiple comparisons (FWE-corrected), with age, gender, and education as covariates. UPDRS-III and MCI status were included as covariates for comparisons between PD-RBD and PD-nRBD subgroups and for correlation analyses. The color bars indicate the *p*-values for between-group differences in cortical thickness, with red-yellow areas representing significant thinning in the first compared to the second group (top line) and blue gradient representing significant negative correlation between cortical thickness and tonic and phasic REM sleep motor activity (bottom line). FWE = family-wise error; MCI = mild cognitive impairment; PD-RBD = Parkinson's disease with REM sleep behavior disorder; PD-nRBD = PD without RBD; UPDRS-III = Unified Parkinson's Disease Rating Scale, Part III.

cortex, extending to the fusiform cortex) (Table 2 and Figure 1). Compared with controls, people with PD-RBD showed extensive bilateral cortical thinning in the frontal, cingulate, temporal, parietal, and occipital regions. People with PD-nRBD showed more restricted cortical thinning bilaterally in the frontal (primarily in the precentral and paracentral cortices with some rostral extension), parietal (superior lobule and precuneus), and occipital (cuneus) regions. No increase in cortical thickness was found in either PD subgroup.

Voxel-based morphometry

People with PD-RBD had reduced local volume in the lingual gyrus/cerebellum compared with people with PD-nRBD (Table 3 and

Figure 2). Compared with controls, people with PD-RBD showed widespread reduction in local volume bilaterally in both cortical (frontal, temporal, parietal, and occipital regions) and subcortical (basal ganglia, thalamus, hippocampus, and cerebellum) structures. Compared with controls, people with PD-nRBD also showed reduced volume, primarily located in the bilateral hippocampus and in the right inferior, middle, and superior temporal regions. No increase in volume was found in either PD subgroup.

Deformation-based morphometry

No significant local differences in contraction or expansion between PD subgroups were found. However, people with PD-RBD showed significant widespread contraction bilaterally in the cortical (frontal, temporal, parietal, and occipital) and subcortical (cerebellum, basal ganglia, thalamus, and brainstem) regions when compared with controls (Table 3 and Figure 2). People with PD-nRBD showed contraction in the right temporal lobe but also in the left temporal lobe and the bilateral parietal and occipital lobes when compared with controls. Clusters in the brainstem that showed abnormal contraction in people with PD-RBD were located within the pontomedullary reticular formation and the midbrain (Figure 3). Less extensive abnormal contraction in the brainstem was also found in people with PD-nRBD in the midbrain and within the basilar pons at the midbrain junction. No significant volume expansion was found in either PD subgroup versus controls.

Subcortical shape analysis

Comparisons between people with PD-RBD and PD-nRBD showed surface contraction in the putamen (41% decrease in the left; 48% in the right) in people with RBD. No shape expansion was found in people with PD-RBD (Figure 4). Compared with controls, people with PD-RBD showed surface contraction in the pallidum (50% of the surface decreased in the left; 42% in the right), putamen (54% of the surface decreased in the left; 88% in the right), right nucleus accumbens (69% of the surface decreased), and left hippocampus (38% of the surface decreased). Compared with controls, people with PD-nRBD showed surface contraction in the pallidum (72% of the surface decreased in the left; 76% in the right), right nucleus accumbens (32% of the surface decreased), and right hippocampus (19% of the surface decreased). No shape expansion was found in either PD subgroup versus controls. Results of the analyses performed with only the 30 controls who underwent PSG were similar to those including the whole

Table 3. Results of voxel-based and deformation-based morphometry

Region with abnormalities*	Hemisphere	Cluster size, mm²	MNI coordinates			*P*
			x	*y*	*z*	
Voxel-based morphometry						
PD-RBD < PD-nRBD						
Lingual gyrus/cerebellum	Left	156	−14	−56	−9	0.030
PD-RBD < Controls						
Lingual gyrus	Left	78 207	−15	−50	−10	<0.001
Putamen	Right	24 278	26	−2	−8	<0.001
Supramarginal gyrus	Left	778	−54	−30	50	0.005
Supramarginal gyrus	Right	231	54	−26	51	0.008
Inferior temporal gyrus	Right	403	50	−28	−22	0.023
Paracentral gyrus	Right	57	2	−27	74	0.026
Medial superior frontal gyrus	Left	479	−9	50	46	0.031
PD-nRBD < Controls						
Fusiform gyrus	Right	3739	45	−38	−18	0.006
Temporal pole	Right	706	33	21	−42	0.017
Amygdala	Right	602	28	−6	−21	0.019
Lateral occipital gyrus	Right	172	27	−86	26	0.020
Amygdala	Left	389	−26	−14	−10	0.023
Lingual gyrus	Right	298	3	−78	−10	0.024
Supramarginal gyrus	Right	193	56	−22	46	0.025
Correlation with % of phasic REM sleep motor activity in PD						
Middle temporal gyrus	Left	454	−60	−62	6	0.018
Deformation-based morphometry						
PD-RBD < Controls						
Cerebellum	Left	144 694	−32	−64	−62	<0.001
PD-nRBD < Controls						
Middle temporal gyrus	Right	48 902	57	−14	−15	0.001
Lateral occipital gyrus	Right	1427	20	−90	20	0.016
Superior parietal lobule	Right	652	26	−66	36	0.036
Supramarginal gyrus	Right	197	62	−21	45	0.041
Correlation with % of phasic REM sleep motor activity in PD						
Middle temporal gyrus	Left	136	−48	−63	9	0.042

Results are corrected for multiple comparisons with FWE at $p < 0.05$ with age, gender, education, and total intracranial volume as covariates. UPDRS-III and MCI status were included as covariates for comparisons between PD-RBD and PD-nRBD subgroups.

FWE = family-wise error; MCI = mild cognitive impairment; MNI = Montreal Neurological Institute; PD-RBD = Parkinson's disease with REM sleep behavior disorder; PD-nRBD = PD without RBD; UPDRS-III = Unified Parkinson's Disease Rating Scale, Part III.

*Labels correspond to the location of the cluster's peak voxel.

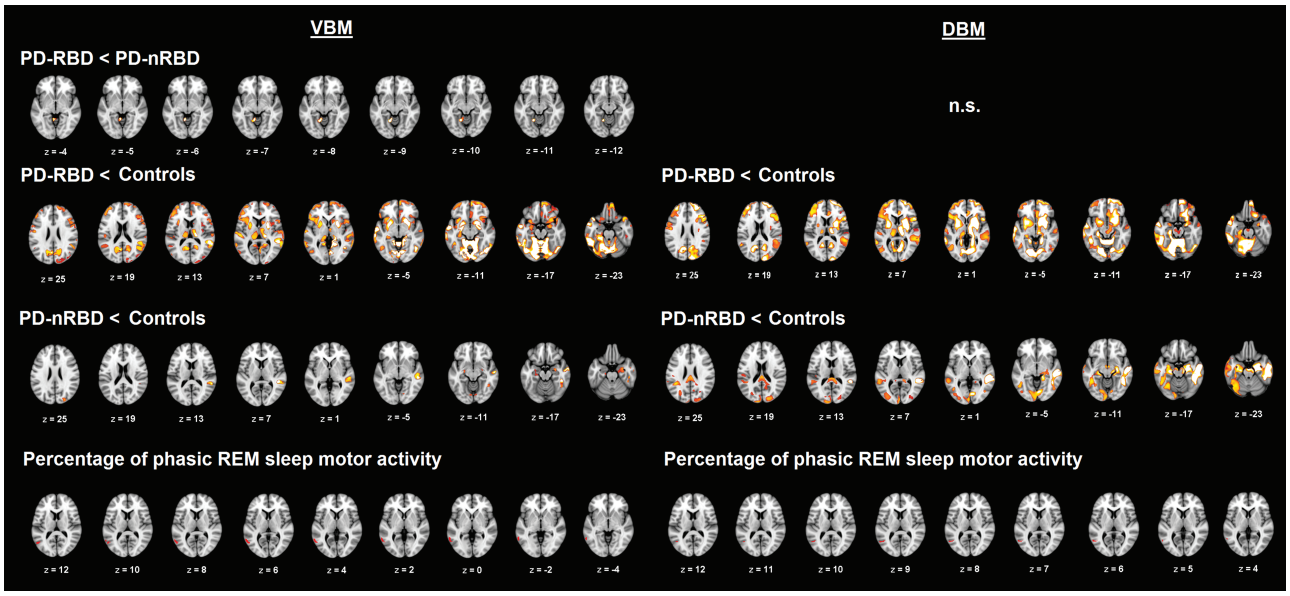

Figure 2. Results of volume abnormalities using voxel-based and deformation-based morphometry. Volume abnormalities between PD-RBD and PD-nRBD (first row), between PD subgroups and controls (second and third rows), and correlations between local volume and percentage of phasic REM sleep motor activity in people with PD (fourth row) are presented. Voxel-based results are presented on the left and deformation-based results on the right. The DBM contrast between PD subgroups did not reveal any significant differences. Results are displayed at $p < 0.05$ corrected for multiple comparisons (FWE-corrected), with age, gender, and education as covariates. UPDRS-III and MCI status were also included as covariates for the comparison between PD-RBD and PD-nRBD subgroups and for correlation analyses. The color bars indicate the –log *p*-values for between-group differences in volume between 1.3 in red ($p < 0.05$ FWE-corrected) and 3 in yellow ($p < 0.001$ FWE-corrected). Significant clusters resulting from correlation analyses with REM sleep motor activity in PD are marked in red only for display purposes. FWE = family-wise error; MCI = mild cognitive impairment; n.s. = not significant; PD-RBD = Parkinson's disease with REM sleep behavior disorder; PD-nRBD = PD without RBD; UPDRS-III = Unified Parkinson's Disease Rating Scale, Part III.

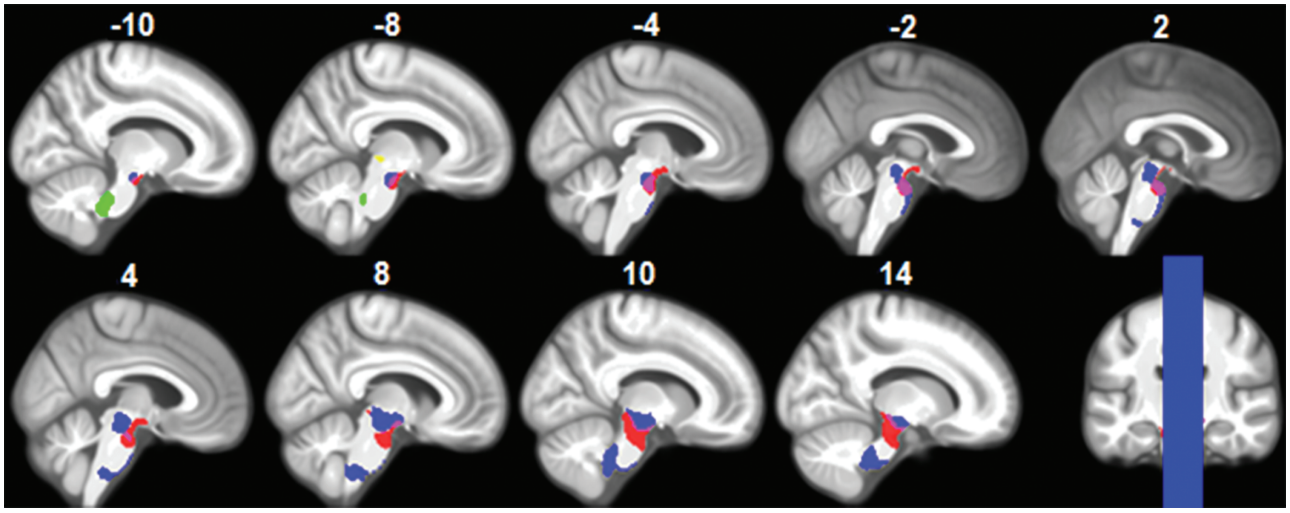

Figure 3. Results of deformation-based morphometry in the brainstem. Clusters of local contraction in PD-RBD vs controls were found within the pontomedullary reticular formation (green and blue clusters) and the midbrain tegmentum (blue, yellow, and pink clusters). Local contraction in PD-nRBD vs controls was found in the midbrain and within the basilar pons at the midbrain junction (red cluster). Results are presented at $p < 0.05$ corrected for multiple comparisons (FWE), with age, gender, education, UPDRS-III, and MCI status as covariates. FWE = family-wise error; MCI = mild cognitive impairment; PD-RBD = Parkinson's disease with REM sleep behavior disorder; PD-nRBD = PD without RBD; UPDRS-III = Unified Parkinson's Disease Rating Scale, Part III.

sample of 41 controls, with some additional shape contraction found in the left nucleus accumbens (21% decrease) in people with PD-RBD versus controls.

Subcortical volumetric analysis

There was a significant effect of group on the normalized subcortical volumes between PD-RBD, PD-nRBD, and controls ($V = 0.601$, $F(28,104) = 1.596$, $p = 0.047$). Subsequent ANCOVAs showed that only volume differences in the left putamen ($p = 0.001$) and the right putamen ($p < 0.001$) survived correction for multiple comparisons. Post hoc tests revealed that people with PD-RBD had lower volume in the left and right putamen compared with people with PD-nRBD ($p = 0.001$) and controls ($p = 0.001$ and $p < 0.001$, respectively). When MCI status and UPDRS-III total score were also added as covariates in the model, people with PD-RBD still had lower volume in the left putamen ($p = 0.0032$) compared with people with PD-nRBD but

only a statistical trend was now found in the right putamen ($p = 0.0078$). Mean normalized volumes of subcortical structures are presented in Table 4.

Regressions with EMG activity during REM sleep

On the cortical level, higher percentage of tonic REM sleep motor activity in people with PD was associated with extensive bilateral thinning in the frontal, parietal, temporal, and occipital cortices (Figure 1). Higher percentage of phasic REM sleep motor activity was associated with more restricted thinning in the left temporal pole and entorhinal cortex, lateral anterior temporal cortex, insula, inferior parietal lobule, and sensorimotor cortex, and in the right precentral cortex (Figure 1). On the subcortical level, higher percentage of tonic REM sleep motor activity was also correlated with shape contraction (39%) in the left thalamus, and with shape expansion (14%) in the right pallidum (Figure 4). Moreover, higher percentage of phasic REM sleep motor activity was associated with reduced local volume and contraction in the posterior middle temporal lobe (Figure 2) and with shape contraction (56% of the surface) in the left thalamus (Figure 4).

Discussion

Using surface-based cortical thickness analysis, VBM, DBM, and subcortical shape and volume analyses, we performed whole-brain mapping of cortical and subcortical tissues to detect structural abnormalities related to RBD in people with PD. The presence of RBD in PD was associated with major alterations in several cortical and subcortical structures. More specifically, people with PD-RBD showed cortical thinning in several cortical regions (i.e. mainly the right perisylvian areas and the inferior temporal cortex extending posteriorly to the fusiform cortex), reduced volume in the left putamen, and surface contraction in both putamina compared to people with PD-nRBD. Both PD subgroups also showed cortical thinning, reduced volume, and shape contraction in cortical and subcortical structures (including the brainstem) compared with controls, with more severe and extended alternations in people

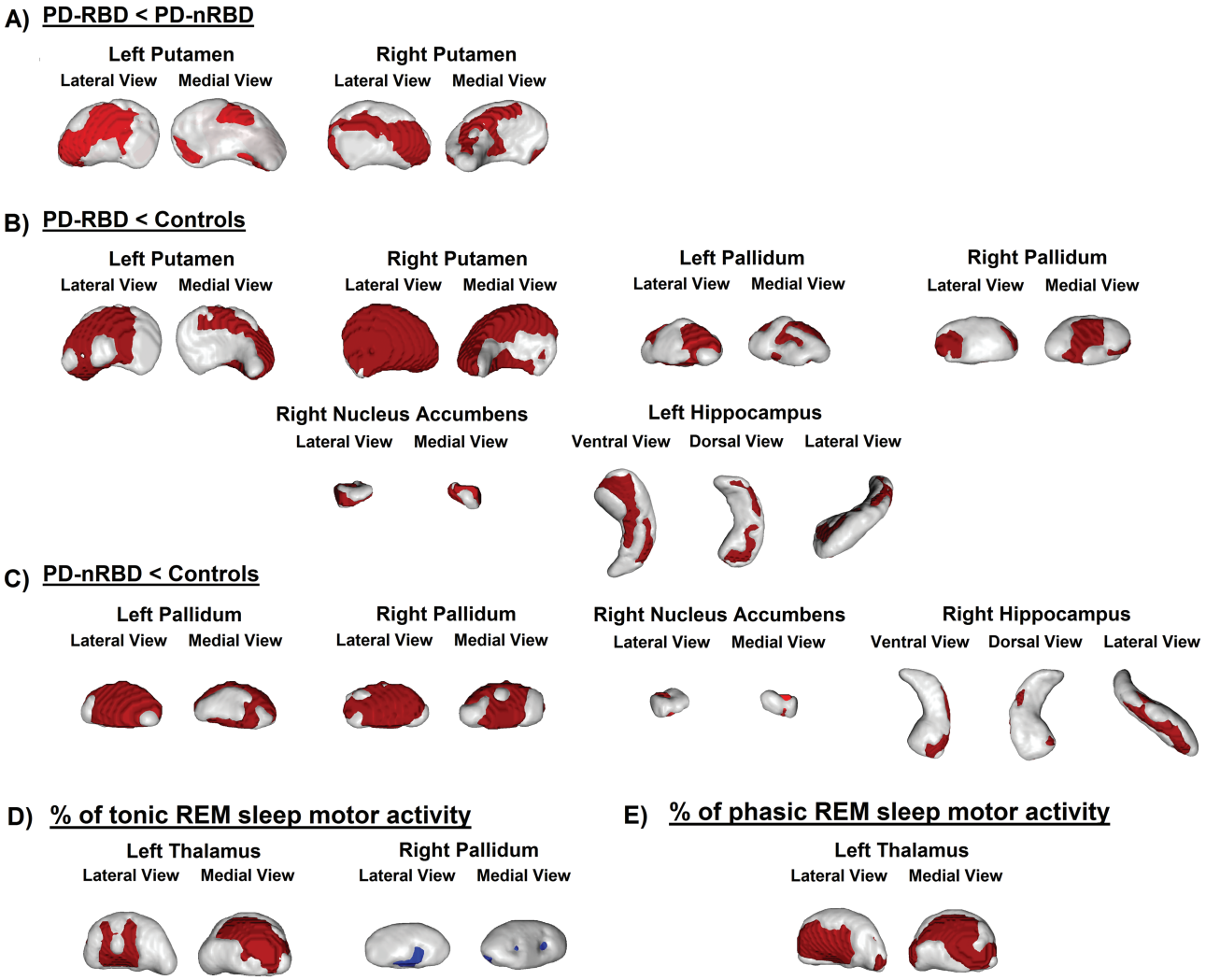

Figure 4. Results of vertex-based subcortical shape analysis. Shape contraction (red) in PD-RBD vs PD-nRBD (A), PD-RBD vs controls (B), and PD-nRBD vs controls (C). Correlations between vertex-based shape and percentage of tonic REM sleep motor activity (D) and percentage of phasic REM sleep motor activity (E) in people with PD (red areas represent negative associations and blue areas represent positive associations). Results are presented at $p < 0.05$ corrected for multiple comparisons (FWE), with age, gender, and education as covariates. UPDRS-III and MCI status were included as covariates for comparisons between PD-RBD and PD-nRBD subgroups. FWE = family-wise error; MCI = mild cognitive impairment; PD-RBD = Parkinson's disease with REM sleep behavior disorder; PD-nRBD = PD without RBD; UPDRS-III = Unified Parkinson's Disease Rating Scale, Part III.

Table 4. Mean normalized volumes of subcortical structures between participants

Hemisphere	Structure	PD-RBD	PD-nRBD	Controls
Left	Amygdala	1822.9 (430.9)	1915.7 (274.5)	1824.9 (259.4)
	Caudate nucleus	4023.6 (568.0)	4382.2 (576.5)	4318.9 (365.7)
	Hippocampus	4585.9 (753.2)	5064.3 (663.3)	5140.1 (654.1)
	Nucleus accumbens	583.6 (141.8)	688.0 (110.9)	691.3 (105.0)
	Pallidum	2185.6 (295.6)	2271.8 (207.6)	2408.9 (400.4)
	Putamen	5585.2 (527.8)	6417.6 (632.5)	6350.1 (584.6)
	Thalamus	9553.8 (998.2)	10453.9 (859.5)	10205.6 (792.5)
Right	Amygdala	1848.6 (278.5)	1944.1 (354.3)	1928.8 (293.8)
	Caudate nucleus	4344.2 (560.8)	4600.2 (541.0)	4505.5 (360.0)
	Hippocampus	4857.8 (568.0)	5091.9 (793.2)	5291.9 (644.7)
	Nucleus accumbens	430.2 (148.6)	544.3 (140.6)	557.6 (121.2)
	Pallidum	2254.8 (215.5)	2350.7 (314.8)	2515.0 (422.1)
	Putamen	5618.2 (621.9)	6408.7 (663.6)	6582.2 (524.3)
	Thalamus	9458.6 (893.3)	10123.6 (796.5)	9932.1 (858.8)

Mean volumes are given in mm^3 (standard deviation).
PD-RBD = Parkinson's disease with REM sleep behavior disorder; PD-nRBD = PD without RBD.

with PD-RBD. In people with PD as a whole group, REM sleep motor activity was associated with extensive cortical thinning, reduced temporal volume, and shape contraction in the left thalamus. These results provide some neuroanatomical explanations for the more severe and aggressive clinical phenotype reported in people with PD with concomitant RBD.

To date, only a few VBM studies have investigated gray matter in relation to RBD in PD, with varying results [7–11]. The most consistent finding was volume decrease in the temporal lobes in PD-RBD compared with people with PD-nRBD [8, 10, 11], which we also found. Elsewhere, either local volume changes were found in the cingulate and posterior regions [10, 11] and in the thalamus [7] in PD-RBD compared with people with PD-nRBD, or else no between-group differences were obtained [9]. Another study used DBM and found volume decreases in several subcortical (brainstem, cerebellum, diencephalon, striatum, and limbic system) and cortical (anterior cingulate) regions and volume increases in olfactory cortical regions in PD-RBD compared with people with PD-nRBD [13]. Our results are in line with this study as our findings using DBM reveal a very extensive and diffuse pattern of abnormal contraction. However, some of the previous studies used screening questionnaires to identify RBD in PD populations [10, 11, 13], possibly resulting in misclassification. PSG is mandatory for RBD diagnosis in order to identify RSWA, confirm the presence of motor behaviors during REM sleep, and exclude other sleep disorders such as sleep apnea or sleepwalking [1]. Other limitations included the use of statistical thresholds uncorrected for multiple comparisons [8, 10, 11] and absence of controls [10]. Moreover, all these studies investigated volume only (using VBM and DBM). In this study, we used surface-based cortical thickness and vertex-based subcortical shape analyses for the first time to unveil structural alterations associated with RBD in people with PD. In people with idiopathic RBD, these techniques were shown to reveal additional structural changes in comparison to volume-based techniques [14, 15, 31], suggesting that surface- and volume-based techniques should be used complementarily when investigating RBD-related structural changes. DBM allows for the direct estimation of local volume changes in both gray and white matter by generating Jacobian fields [26]. In the present study and Boucetta et al.'s study [13], extensive volume contraction was found in cortical and subcortical regions, including the brainstem, suggesting white matter alterations in people with PD-RBD and, to a lesser extent, in people with PD without RBD. However, DBM does not inform on the nature of the changes in white matter. Studies using diffusion tensor imaging in people with PD with and without RBD found no differences that survived correction for multiple comparisons [9–11]. Future studies should investigate diffusion-weighted metrics to better understand the pathophysiological mechanisms in white matter.

RBD is a frequent nonmotor feature of PD, ranging from 33% to 46% according to studies that used PSG for RBD diagnosis [2, 3]. As mentioned above, the presence of RBD in PD is associated with more severe symptoms, poorer prognostics, and cerebral functional alterations, and is one of the strongest markers of a "diffuse malignant" subtype of PD [4, 5, 32]. People with PD-RBD showed poorer cognitive performance and higher MCI frequency, and RBD is among the strongest predictors of dementia in PD [6, 33, 34]. In some, but not all studies, people with PD-RBD also showed more motor alterations, including predominance of the akineto-rigid form, lower levodopa responsiveness, more severe gait freezing, and higher fall frequency [32]. These clinical differences are associated with diffuse EEG slowing during wakefulness [35], decreased cholinergic innervation in neocortical, thalamic, and limbic cortical regions [36], decreased nigrostriatal dopaminergic activity in the caudate [37], decreased metabolism in posterior cortical regions, and increased metabolism in anterior regions [37]. In this study, we controlled for several covariates potentially related to structural abnormalities in PD such as motor symptoms and cognitive status. Other covariates associated with structural integrity should have been considered, such as postural instability and gait disorder (PIGD); however, our protocol did not include specific assessment of these variables. Our findings suggest some explanation for the clinical symptoms and brain functional abnormalities found in the PD with RBD phenotype.

In this study, REM sleep motor activity in people with PD was associated with contraction in the left thalamus, extensive cortical thinning, and subtle volume loss in the temporal lobe, particularly in relation to tonic REM sleep motor activity. No correlations were found in brainstem regions known to play a role in REM sleep muscle atonia [38]. This contributes to our understanding of the bases of RSWA in RBD, alongside another

study that found an association between RSWA and reduced signal intensity in the locus coeruleus and pre-coeruleus complex using neuromelanin-sensitive MRI imaging, a method not used in the present study [9]. The thalamus is involved in REM sleep regulation via strong glutamatergic connections with the sublaterodorsal tegmental nucleus and cholinergic connections with the pedunculopontine nucleus, which send descending projections to medullar motor centers [39, 40]. Projections between the pedunculopontine nucleus and the thalamus degenerate in PD [41], and more prominently when patients report RBD symptoms [36]. An abnormally shaped thalamus may therefore relate to ongoing pathology within these structures. Unlike a previous study [7], we did not find significantly reduced volume or abnormal shape in the thalamus in PD-RBD compared to people with PD-nRBD. This may be due to differences between our PD populations. Indeed, in the previous study [7], people with PD were older, more heterogeneous in terms of disease duration, and with more motor impairment (higher UPDRS-III scores) than in our study. However, in the present study, we did find that people with PD-RBD had significantly reduced local volume in the bilateral thalamus in comparison to controls, a finding that was not present in people with PD-nRBD. In addition, the fact that the thalamic shape relates significantly to RSWA, while not being different between PD subgroups, may be due to the high variability in REM sleep motor activity in patients. Whereas a regression approach allowed investigating the structural correlates of RSWA by taking into account the variability in REM sleep motor activity between patients, the between-group approach used cutoff scores to qualify REM sleep motor activity in PD-RBD and PD-nRBD as abnormal or not without further consideration of the extent of motor activity. As for the sensorimotor and anterior temporal regions in RSWA, their implication remains to be understood. However, cortical thinning in these regions is associated with CSF total alpha-synuclein levels in people with idiopathic RBD [42]. Our study also concurs with the cortical regions showing more synuclein deposition in people with PD with versus without probable RBD [43]. Moreover, RSWA in PD has been related to disease severity and poorer cognitive performance [6, 34]. In idiopathic RBD, tonic REM sleep motor activity predicts conversion to PD [44]. Therefore, our results may represent cortical regions that are more vulnerable to neurodegeneration in PD.

Our results are also in line with the Unified Staging System for Lewy Body Disorders (USSLB) [45]. According to the USSLB, synuclein depositions are initially found in the olfactory bulb (stage I), which then spread following pathways of propagation in which depositions become more predominant in the brainstem (stage IIa) or in the limbic areas (stage IIb). At stage III, involvement of the brainstem and limbic regions becomes fairly equal and at stage IV, synuclein depositions spread through the neocortex. Our results show that both people with PD with and without RBD have structural abnormalities that correspond to a stage IV involvement. In people with PD-RBD, extensive volume abnormalities were found throughout the cortical mantle. In contrast, people with PD-nRBD showed less extensive abnormalities, with changes being prominent in the right temporal lobe and extending to more posterior regions in terms of thinning and reduced volume. Moreover, both PD subgroups showed hippocampal and brainstem abnormalities (the latter more extensive in people with PD-RBD), which concur with a neocortical involvement beyond stage III. Brainstem structural impairments are in line with the abnormal contraction and reduced signal intensity found in PD with RBD [9, 13]. Similarly to previous studies, no brainstem volume changes were detected in PD using VBM only [7, 9–11], suggesting that DBM allows detecting brainstem changes associated with RBD in PD. Despite some pathological evidence showing greater range and density of synuclein deposition in people with PD with RBD versus people with PD without RBD, including in the brainstem [43], the extent to which brainstem deformation actually refers to pathological changes remains to be investigated in this population. In terms of the regions surrounding the nigrostriatal pathway, which is thought to underlie the motor symptoms in PD [46], both PD subgroups showed structural abnormalities in the basal ganglia versus controls, which were more severe in the putamen for people with PD-RBD. This agrees with findings of reduced volume in the putamen in PD-RBD [13] and abnormal shape in the putamen in people with PD overall [47], the latter associating with motor symptoms [48]. This also concurs with the abnormal contraction in the lenticular nucleus in people with idiopathic RBD [15, 31]. Therefore, our neuroimaging results support the idea that the RBD phenotype in PD corresponds to more advanced brain neurodegeneration, in line with a recent study showing that the presence of RBD predicts motor and cognitive progression in people with PD with greater synuclein, amyloid, and dopaminergic pathology [49]. Neurodegeneration in PD has also been proposed to result from a disease-spreading process during which misfolded proteins propagate through intrinsic networks present in healthy brains [50]. Cortical thickness investigation has recently supported the network propagation hypothesis in PD, with thinning being found in cortical regions showing greater structural or functional connectivity to the subcortical disease reservoir [51]. This hypothesis is also in line with our pattern of results in people with PD: cortical thinning in the sensorimotor cortex in both PD subgroups may come from the spread of pathology from the basal ganglia through corticopetal systems, which concurs with both subgroups (but more so for people with PD-RBD) showing subcortical abnormalities. However, further research on disease spread mechanisms is needed to support this hypothesis.

Some limitations should be noted in this study. Despite our patients having undergone thorough clinical assessment, PD subgroups were relatively small. This may have affected the statistical power of our analyses and may explain the lack of significant volume differences between PD subgroups. Moreover, although we controlled for motor symptoms and cognitive status, other confounders of interest could not be taken into account (e.g. PIGD subtype or gait freezing symptoms).

In conclusion, the presence of RBD in PD is associated with extensive cortical and subcortical alterations, with higher REM sleep motor activity being correlated with thalamic contraction, extensive cortical thinning, and subtle temporal volume loss.

Funding

This work was supported by the Canadian Institutes of Health Research, the Fonds de Recherche du Québec – Santé, and The W. Garfield Weston Foundation. Dr. J.-F. Gagnon holds a Canada Research Chair in Cognitive Decline in Pathological Aging.

Conflict of interest statement. S. Rahayel reports no disclosures. M. Gaubert reports no disclosures. Dr. R. B. Postuma reports grants and personal fees from the Fonds de Recherche du Québec

– Santé (FRQ-S), the Canadian Institutes of Health Research (CIHR), The Parkinson Society of Canada, The W. Garfield Weston Foundation, The Michael J. Fox Foundation, The Webster Foundation, and personal fees from Roche/Prothena, Teva Neurosciences, Novartis Canada, Biogen, Boehringer Ingelheim, Theranexus, Takeda, Jazz Pharmaceuticals, Abbvie, Jannsen, and GE HealthCare, outside the submitted work. Dr. J. Montplaisir received research grants from The Parkinson Society of Canada, the CIHR, The W. Garfield Weston Foundation and personal compensation for consultancy services from Takeda, Merck, and Canopy International. Dr. J. Carrier reports research funding from the CIHR, RANA, Merck Canada, and Respironics. Dr. O. Monchi reports funding from the CIHR, the Natural Sciences and Engineering Research Council of Canada (NSERC), and the Canadian Fund for Innovation. He holds a Canada Research Chair in Non-motor Symptoms of Parkinson's Disease and the Tourmaline Oil Chair in Parkinson's Disease. D. Rémillard-Pelchat reports no disclosures. P.-A. Bourgouin reports no disclosures. Dr. M. Panisset has received research support from Medtronic and he serves on advisory boards for Allergan and Merz. Dr. S. Chouinard has received research support from Abbvie. Dr. S. Joubert received funding from the FRQ-S, the CIHR, and the Alzheimer Society of Canada. Dr. J.-F. Gagnon received grants from The W. Garfield Weston Foundation, the CIHR, The Parkinson Society of Canada, and the FRQ-S. He holds a Canada Research Chair in Cognitive Decline in Pathological Aging.

References

1. American Academy of Sleep Medicine. *The International Classification of Sleep Disorders — Third Edition (ICSD-3)*. Darien, IL: American Academy of Sleep Medicine; 2014.
2. Gagnon JF, *et al*. REM sleep behavior disorder and REM sleep without atonia in Parkinson's disease. *Neurology*. 2002;**59**(4):585–589.
3. Sixel-Döring F, *et al*. Associated factors for REM sleep behavior disorder in Parkinson disease. *Neurology*. 2011;**77**(11):1048–1054.
4. Fereshtehnejad SM, *et al*. New clinical subtypes of Parkinson disease and their longitudinal progression: a prospective cohort comparison with other phenotypes. *JAMA Neurol*. 2015;**72**(8):863–873.
5. Fereshtehnejad SM, *et al*. Clinical criteria for subtyping Parkinson's disease: biomarkers and longitudinal progression. *Brain*. 2017;**140**(7):1959–1976.
6. Jozwiak N, *et al*. REM sleep behavior disorder and cognitive impairment in Parkinson's disease. *Sleep*. 2017;**40**(8):zsx101.
7. Salsone M, *et al*. Reduced thalamic volume in Parkinson disease with REM sleep behavior disorder: volumetric study. *Parkinsonism Relat Disord*. 2014;**20**(9):1004–1008.
8. Kim HJ, *et al*. Brain atrophy of secondary REM-Sleep behavior disorder in neurodegenerative disease. *J Alzheimers Dis*. 2016;**52**(3):1101–1109.
9. García-Lorenzo D, *et al*. The coeruleus/subcoeruleus complex in rapid eye movement sleep behaviour disorders in Parkinson's disease. *Brain*. 2013;**136**(Pt 7):2120–2129.
10. Ford AH, *et al*. Rapid eye movement sleep behavior disorder in Parkinson's disease: magnetic resonance imaging study. *Mov Disord*. 2013;**28**(6):832–836.
11. Lim JS, *et al*. Neural substrates of rapid eye movement sleep behavior disorder in Parkinson's disease. *Parkinsonism Relat Disord*. 2016;**23**:31–36.
12. Borghammer P, *et al*. A deformation-based morphometry study of patients with early-stage Parkinson's disease. *Eur J Neurol*. 2010;**17**(2):314–320.
13. Boucetta S, *et al*. Structural Brain Alterations Associated with Rapid Eye Movement Sleep Behavior Disorder in Parkinson's Disease. *Sci Rep*. 2016;**6**:26782.
14. Rahayel S, *et al*. Patterns of cortical thinning in idiopathic rapid eye movement sleep behavior disorder. *Mov Disord*. 2015;**30**(5):680–687.
15. Rahayel S, *et al*. Abnormal gray matter shape, thickness, and volume in the motor cortico-subcortical loop in idiopathic rapid eye movement sleep behavior disorder: association with clinical and motor features. *Cereb Cortex*. 2018;**28**(2):658–671.
16. Patenaude B, *et al*. A Bayesian model of shape and appearance for subcortical brain segmentation. *Neuroimage*. 2011;**56**(3):907–922.
17. Hutton C, *et al*. A comparison between voxel-based cortical thickness and voxel-based morphometry in normal aging. *Neuroimage*. 2009;**48**(2):371–380.
18. Postuma RB, *et al*. MDS clinical diagnostic criteria for Parkinson's disease. *Mov Disord*. 2015;**30**(12):1591–1601.
19. American Psychiatric Association. *Diagnostic and Statistical Manual of Mental Disorders: DSM-5*. Washington, D.C.: American Psychiatric Association; 2013.
20. Montplaisir J, *et al*. Polysomnographic diagnosis of idiopathic REM sleep behavior disorder. *Mov Disord*. 2010;**25**(13):2044–2051.
21. Iber C, *et al*. *The AASM Manual for the Scoring of Sleep and Associated Events: Rules, Terminology and Technical Specifications*. Westchester, IL: American Academy of Sleep Medicine; 2007.
22. Goetz CG, *et al*.; Movement Disorder Society UPDRS Revision Task Force. Movement Disorder Society-sponsored revision of the Unified Parkinson's Disease Rating Scale (MDS-UPDRS): scale presentation and clinimetric testing results. *Mov Disord*. 2008;**23**(15):2129–2170.
23. Broadbent DE, *et al*. The Cognitive Failures Questionnaire (CFQ) and its correlates. *Br J Clin Psychol*. 1982;**21 (Pt 1)**:1–16.
24. Litvan I, *et al*. Diagnostic criteria for mild cognitive impairment in Parkinson's disease: movement disorder society task force guidelines. *Mov Disord*. 2012;**27**(3):349–356.
25. Gagnon JF, *et al*. Mild cognitive impairment in rapid eye movement sleep behavior disorder and Parkinson's disease. *Ann Neurol*. 2009;**66**(1):39–47.
26. Gaser C, *et al*. Deformation-based morphometry and its relation to conventional volumetry of brain lateral ventricles in MRI. *Neuroimage*. 2001;**13**(6 Pt 1):1140–1145.
27. Smith SM, *et al*. Accurate, robust, and automated longitudinal and cross-sectional brain change analysis. *Neuroimage*. 2002;**17**(1):479–489.
28. Smith SM, *et al*. Advances in functional and structural MR image analysis and implementation as FSL. *Neuroimage*. 2004;**23** (Suppl 1):S208–S219.
29. Smith SM, *et al*. Threshold-free cluster enhancement: addressing problems of smoothing, threshold dependence and localisation in cluster inference. *Neuroimage*. 2009;**44**(1):83–98.
30. Winkler AM, *et al*. Permutation inference for the general linear model. *Neuroimage*. 2014;**92**:381–397.
31. Rahayel S, *et al*. Cortical and subcortical gray matter bases of cognitive deficits in REM sleep behavior disorder. *Neurology*. 2018;**90**(20):e1759–e1770.

32. Kim Y, *et al*. REM sleep behavior disorder portends poor prognosis in Parkinson's disease: a systematic review. *J Clin Neurosci*. 2018;**47**:6–13.
33. Postuma RB, *et al*. Rapid eye movement sleep behavior disorder and risk of dementia in Parkinson's disease: a prospective study. *Mov Disord*. 2012;**27**(6):720–726.
34. Nomura T, *et al*. Clinical significance of REM sleep behavior disorder in Parkinson's disease. *Sleep Med*. 2013;**14**(2):131–135.
35. Gagnon JF, *et al*. Association between waking EEG slowing and REM sleep behavior disorder in PD without dementia. *Neurology*. 2004;**62**(3):401–406.
36. Kotagal V, *et al*. Symptoms of rapid eye movement sleep behavior disorder are associated with cholinergic denervation in Parkinson disease. *Ann Neurol*. 2012;**71**(4):560–568.
37. Arnaldi D, *et al*. Functional neuroimaging and clinical features of drug naive patients with de novo Parkinson's disease and probable RBD. *Parkinsonism Relat Disord*. 2016;**29**:47–53.
38. McKenna D, *et al*. Degeneration of rapid eye movement sleep circuitry underlies rapid eye movement sleep behavior disorder. *Mov Disord*. 2017;**32**(5):636–644.
39. Martinez-Gonzalez C, *et al*. Topographical organization of the pedunculopontine nucleus. *Front Neuroanat*. 2011;**5**:22.
40. Valencia Garcia S, *et al*. Genetic inactivation of glutamate neurons in the rat sublaterodorsal tegmental nucleus recapitulates REM sleep behaviour disorder. *Brain*. 2017;**140**(2):414–428.
41. Kotagal V, *et al*. Thalamic cholinergic innervation is spared in Alzheimer disease compared to parkinsonian disorders. *Neurosci Lett*. 2012;**514**(2):169–172.
42. Compta Y, *et al*. Correlates of cerebrospinal fluid levels of oligomeric- and total-α-synuclein in premotor, motor and dementia stages of Parkinson's disease. *J Neurol*. 2015;**262**(2):294–306.
43. Postuma RB, *et al*. REM sleep behavior disorder and neuropathology in Parkinson's disease. *Mov Disord*. 2015;**30**(10):1413–1417.
44. Postuma RB, *et al*. Severity of REM atonia loss in idiopathic REM sleep behavior disorder predicts Parkinson disease. *Neurology*. 2010;**74**(3):239–244.
45. Adler CH, *et al*. Neuropathological basis of nonmotor manifestations of Parkinson's disease. *Mov Disord*. 2016;**31**(8):1114–1119.
46. Braak H, *et al*. Staging of brain pathology related to sporadic Parkinson's disease. *Neurobiol Aging*. 2003;**24**(2):197–211.
47. Sterling NW, *et al*. Structural imaging and Parkinson's disease: moving toward quantitative markers of disease progression. *J Parkinsons Dis*. 2016;**6**(3):557–567.
48. Nemmi F, *et al*. Parkinson's disease and local atrophy in subcortical nuclei: insight from shape analysis. *Neurobiol Aging*. 2015;**36**(1):424–433.
49. Pagano G, *et al*. REM behavior disorder predicts motor progression and cognitive decline in Parkinson disease. *Neurology*. 2018;**91**(10):e894–e905.
50. Zeighami Y, *et al*. Network structure of brain atrophy in de novo Parkinson's disease. *Elife*. 2015;**4**:e08440.
51. Yau Y, *et al*. Network connectivity determines cortical thinning in early Parkinson's disease progression. *Nat Commun*. 2018;**9**(1):12.